論 文

Time Effects on Cu-Zn-Al Shape Memory Alloys

Vicenç Torra*, Antoni Isalgue* and Henri Tachoire**

(Received May 5, 1997)

Reliability is a critical word in industrial applications of Shape Memory Alloys (SMA) usually called smart materials. Applications of these materials require a rigorous stability of the transformation temperatures and a small hysteresis. The applications of the SMA to the continuous actuators involve a time guarantee about the constructed devices related to the suitable composition and heat treatment. From a mechanical model for a single martensite plate, the shape of the hysteresis cycle (single crsytal of Cu-Zn-Al alloys) is obtained by generalizing the representation to N plates. The observed time effects on the hysteresis loops related to diffusion processes were also taken into account. They allow to explain the martensite recoverable creep and the micromemory effects. Using high resolution on resistance measurements, the room temperature effects on the parent phase acting over the transformation temperature Ms is evaluated. The effect produced by two atomic order parameters (*i.e.* B2 and $L2_1$) related to the yearly room temperature evolution (for instance, summer to winter) induces predictive evolution of transformation temperature and the mean uncertainty reduces drastically ($\delta M_s \approx \pm 0.05$).

1. Introduction

Smart materials carry out simultaneous functions as sensors and actuators. One of them, the memory alloys are distinguished by a martensitic transformation between metastable phases [see, 1-9 as general references]. The high temperature crystallographic form (or austenite) is coherent with a large number of variants in the low temperature structure (or martensite). This allows for various macroscopic shapes in the low temperature phase to coexist with only one high temperature shape (Shape Memory Effect). Only in a highly particular situation the reverse process produces new orientation.[10]

The main interest on continuous actuators focuses only in the coexistence domain (from 0 to 100 per cent of martensite phase) and in small hysteresis as copper based alloys. The industrial interest needs an experimental method classifying the ability of available alloys. Recent improvements relate with the availability of appropriate stored data or representative models.[11-15] Likewise, physical image models have been built for single crystals, starting from the detailed behaviour of single variant martensite domains or plates.[16-19] Recently, numerical routines have been established for the construction of devices in SMA [20-21] and some models have been described which include the perturbations introduced by the heat transport towards the surroundings.[22-23]

The applicability of the material for on-off actions need only a poor reliability. Usually, the phase changes are produced by an electrical current pulse and its associated change of temperature is fairly high. To avoid spontaneous changes of the material, it is convenient to use alloys which have a considerable hysteresis. Within this group of applications, TiNi microactuators can be found (see [24] and related references). Recently, techniques for the production of thin films on TiNi have

* CIRG-DFA-ETSECCPB, Polytechnical University of Catalonia, E-08034 Barcelona, Spain
E-mail: vtorra@etseccpb.upc.es
**Laboratoire de Thermochimie Universite de Provence, F-13331 Marseille CEDEX 03, France
E-mail: thchimie@newsup.univ-mrs.fr

been developed by Ar-plasma deposition directly in crystalline form (without ageing at high temperature).[25] In a continuous and smooth control, we need a small hysteresis and the rigorous stability of the transformation temperatures: a time guarantee is required for constructed devices The transformation temperature depends on thermal treatments or, in equivalent form, on the degree of atomic order in the material (see, for instance [7, 26-28] and related references). Recently, it has been detected an increasing interest in the degree of atomic order and its evolution with time.[29-33] A careful analysis (accuracy ± 1 K) of the evolution of the transformation temperature needed to establish the limits of guarantee of the Thermomark can be found in reference 34. This device is used to guarantee the safekeeping of frozen products. The analysis of the experimental results indicates that the transformation temperatures fluctuate "pseudo-randomly" in long term observations within relatively reduced margins ($\Delta M_s \approx \pm 2$ K). In general, the changes in M_s have been associated to many causes: atomic order (B2 and $L2_1$ in Cu-Zn-Al alloys), domains of order, elastic dipoles, dislocations (creation, movement and evolution), ...

In this work, we describe the behaviour of the material with the help of a physical image model (single crystal with one or more single variant). The experimental observations allow the inclusion of the local modifications in the equilibrium temperature produced by the coexistence of the two phases. This permits to explain the phenomena of martensite creep, β recovery, ...By carrying out continuous observations of the electrical resistance in austenite phase and using a rigorous control and programmation of the temperature, it is possible to quantify the behaviour of the material near room temperature. The analysis of the experimental results allows phenomenological rules which regulate the behaviour of the material as functions of time and room temperature. The results establish that the uncontrolled fluctuations of the transformation temperature can be strongly reduced ($\delta M_s \approx \pm 0.05$ K).

2. Coexistence processes: stress-strain-temperature-time

A series of global and partial stress-strain cycles have been carried out using high resolution adapted equipment described elsewhere.[35-38] Cu-Zn-Al single crystals (electronic concentration 1.48 e/a) were used.

The samples were cut with the appropriate crystalographic orientation to obtain the maximum deformation (around 9 per cent) in b.c.c. to monoclinic ($\beta \rightarrow \beta'$). The available transformation length l of used samples is around 4 mm, near 1 mm^2 of the cross section and standard Ms near 280 K. The observations have allowed the visualization of the effects of the nucleation in the martensite phase, the effect of the intrinsic thermoelasticity produced by the interaction of the interphase with the pre-existing dislocations, the friction related to the interphase movements, the coalescence of the martensite limits in the same variant and related phenomena.

A thermomechanical model is described, like the one in page 305 of ref. 39, coherent with the experimental observations of a single martensite plate. The sample is divided in N domains (or plates) of transformation-retransformation. The maximal deformation is 9 per cent (X_{max} = 0.09 ℓ) and the related lengthening for each plate (x_{max}^0) is 0.09 ℓ /N. Increasing the stress or the external force Fext the lengthening x of each plate increases from zero to x_{max}^0. In general, the actual lengthening x is a function of external force, temperature T and previous path or history. The **Fig. 1** visualizes the relevant unloading needed to recover completely the parent phase without thin martensite microplates. In **Fig. 2**, the path of the working point is presented for only one domain avoiding contributions related to classical thermal expansion and elasticity. Trajectory corresponds to the coordinates F-x, to the transformation from the austenitic phase to the martensitic phase and back-ward.[17-19] For instance, in loading, the path

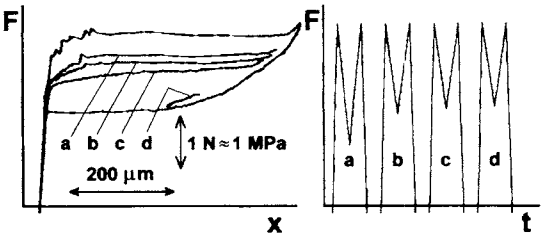

Fig. 1 Experimental hysteretic behavior in single cystal, single variant transformation with several martensite plates. The hysteresis width increases with the achieved unload in internal loop.

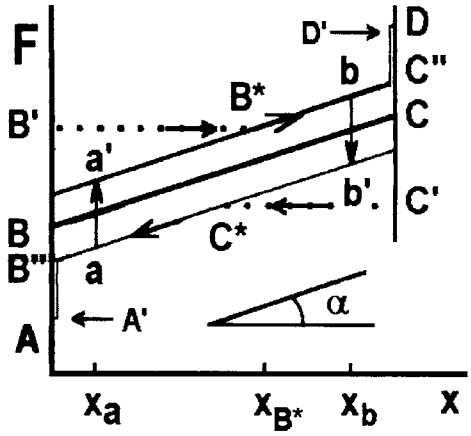

Fig. 2 Model for each martensite plate: trajectory in F (force or stress) against lengthening x.

presented in **Fig.2** correspondig to the i-th plate becomes:

in path AB',

$$F_{ext} < f_{00}^{(i)} + zn_0 + z_{if} \qquad \text{with} \quad x^{(i)} = 0$$

at B' and B* points,

$$F_{ext}^{B'} = F_{ext}^{B*} = f_{00}^{(i)} + z_{if} + \left[\frac{df}{dx}\right] x_{B*} \qquad \text{and} \quad x^{(i)} = x_{B*}$$

at D point,

$$F_{ext}^{D} = f_{00}^{(i)} + z_{if} + \left[\frac{df}{dx}\right] x_{max0} \qquad \text{and} \quad x^{(i)} = x_{max0}$$

in path DC',

$$F_{ext} > f_{00}^{(i)} - zn_1 - z_{if} + \left[\frac{df}{dx}\right] x_{max0} \qquad \text{and} \quad x^{(i)} = x_{max0}$$

On cycling symmetric behavior is used. From austenite to martensite, the path on loading describes A, B, B' (nucleation), B* (after nucleation), C" (only traces of parent phase), D' (complete coalescence with the nearby plate), ...; from martensite to austenite the path describes D, C, C' (b nucleation), C*, B" (unrelevant length), A' (complete disappearance). Path a, a', b, b' is an internal loop with friction related to the movement of interfaces without nucleation; the slope α is a macroscopic effect of the internal thermoelasticity: an interaction between interface and preexistent dislocations. Using a series of N domains, the global and partial (internal loops) hysteresis cycles ***without time effects*** are simulated accurately.[18]

When disturbances on the trajectory of the

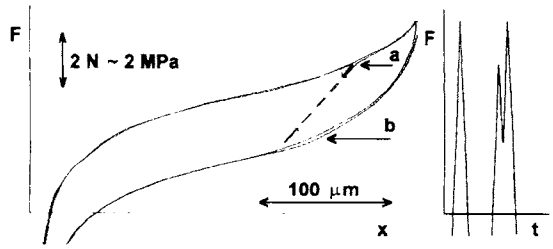

Fig. 3 Left: hysteresis cycle on force F against lengthening x at constant temperature; effect of a force fluctuation (only the extreme points are presented);a) martensite creep; b) "micromemory" effect. Right: force against time (schematic).

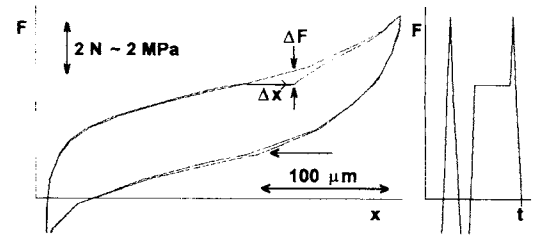

Fig. 4 Left: hysteresis cycle on force F against lengthening x at constant temperature; Δx increase of transformed material at constant load; ΔF related change of load; the arrow indicates the micromemory effect. Right: force against time (schematic).

hysteresis cycle are carried out, it can be observed an increase in the amount of martensite (**Fig. 3**) and a minor micromemory effect. The process could be associated with the reordering of domains by the differences between the frictions from the various martensite plates. This interpretation is insufficient. In fact, martensite creep at constant stress (**Fig. 4**) can be observed. The evolution of the amount of martensite at constant stress (**Fig. 5**(A)) reaches a steady value after approximately 10 hours. The increase can be associated to the coexistence of the two phases and, eventually, to the previous movement of the interphases. The SRC evolution (static recoverable creep) is obtained loading at very low stress rates: the analized point is reached at $ds/dt < 1$ kPa s^{-1}. When the approximation occurs at a greater stress rate (< 10 kPa s^{-1}) an increased creep (DRC or dynamic recoverable creep) is observed. The effects associated with the latent heat are observed for higher stress rates (near 50 kPa s^{-1}). From the series of

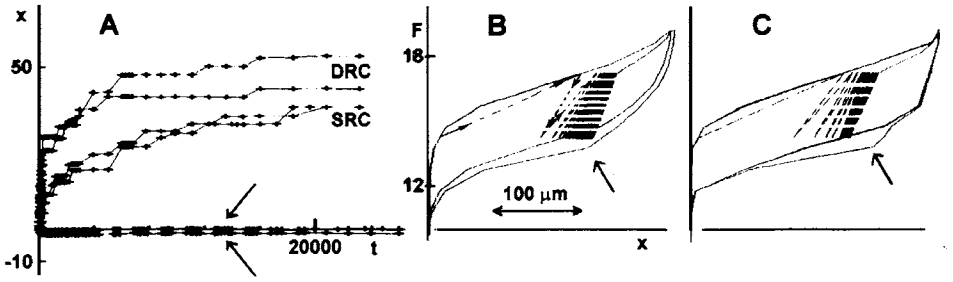

Fig. 5 A) lengthening against time; the arrows indicate the creep effect on unloading; B) experimental: hysteretic behavior with internal loops (only the end points are represented), the arrow indicates the micromemory effect; C) associated simulation. Working temperature used: 290.7 K.

experimental observations, it is derived that the equilibrium temperature T_0 of one or more domains of the sample is affected by the coexistence of the two phases. The SRC and DRC effects are calculated from the value of $\Delta F/\Delta x$, which is determined from **Fig. 4** and the value of $(dF/dT)_{CC}$ (Clausius-Clapeyron equation)*1. The experimental value of $(dF/dT)_{CC}$ is derived from the values of F on homologous points of the hysteresis cycles carried out at different temperatures. The creep effect is a function of the position in the hysteresis cycle. It is lower in the initial part of loading (minor number of active plates) and at the end part (practically no parent phase available). On unloading, reversal of the frictional actions "freezes" the creep effect (see the arrows in **Fig. 5**(A)). During long term observations, several days at constant stress, it is possible to detect a further smaller increase on T_0 probably related with the LTT time evolution on parent phase (see below).

The local evolution of the equilibrium temperature for each plate $\Delta T_0(t)$, can be expressed as [19]:

$$\Delta T_0(t) = \Delta T_0^{SRC}(1-e^{-t/\tau^{SRC}}) + \Delta T_0^{DRC}(1-e^{-t/\tau^{DRC}})$$

$$\Delta T_0^{SRC} = 0.5\ K\ ;\ \Delta T_0^{DRC} = 0.2\ K$$

$$\tau^{SRC} = 6000\ s\ ;\ \tau^{DRC} = 200\ s$$

If the external stress is reduced, the material goes again to β phase, which progressively recovers the initial value of the equilibrium temperature T_0 (β recovery). The observations suggest that the approximation to the reference state follows an exponential form, from the initial value after the previous coexistence process:

$$\Delta T_0^{\beta}(t) = \Delta T_0\, e^{-t/\tau^{\beta}} \quad ;\ \tau_{\beta} \approx 300\ s$$

In **Fig. 5**(B) experimental stress-strain or force-displacement cycles with internal loops are shown. Only the extreme points have been presented in partial cycles. **Fig. 5**(C) is the corresponding computer simulation. The arrows indicate the appearance of the micromemory effect in unloading.

3. Time evolution on parent phase

Computer controlled electrical resistance measurement system which allows a resolution and reproducibility of around 0.05 % (stress free) has been used. Continuous observations have been carried out during more than 3 years with the temperature controlled. Starting from several temperatures T in a steady state, cooling to martensite (263 K) and subsequent heating produces a complete cycle of the transformation-retransformation and the Ms value can be determined from the experimental cycle $R = R(T)$. The sample used (Cu-Zn-Al) has an electronic concentration 1.48 e/a, and the nominal M_s arounds 270 K.

In **Fig. 6**(A), the evolution of the electrical resistance at 293 K (in parent phase) can be observed after soldering the wires on the sample. A general decrease is noted, which fluctuates according to the type of immediate action carried out; microflash heating in the b point (temperature 348 K), 10 hours in the c point, cycling process in d, heating at 363 K by 1 hour in e point, ageing at 365 K by 12 hours in f point and similar to c in g point. The decrease of the resistance is

*1) Fatigue test using INSTRON's equipment and higher stress rates (cycling at 0.8 Hz) produces similar but increased effects as greather as 10 K.[40]

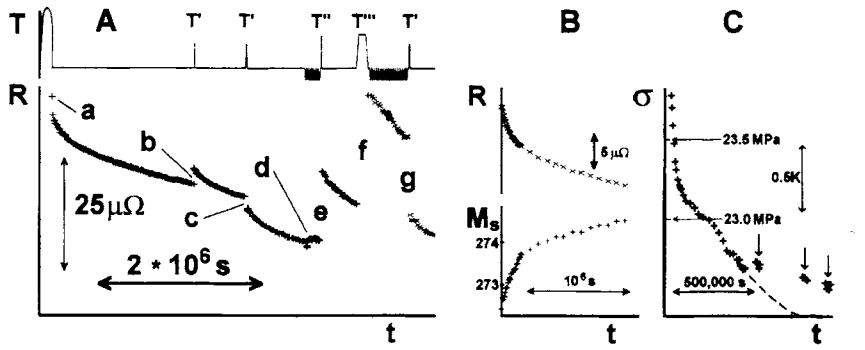

Fig. 6 A-top) temperature against time (schematic); A-bottom) resistance versus time with the action of several micro heat treatments; B) resistance R and transformation temperature MS against time using two cycling frequences; C) critical stress vs. time, - - - - expected evolution; arrows indicates the actual values after several days without cycling.

associated to an increase in the transformation temperature and the process speeds up when cycling. In **Fig. 6** (B), it can be observed the evolution of the resistance and that of M_S for two cycling rates after a microheating. The evolution process of the equilibrium temperature is similar if the system is maintained at a constant temperature and the transformation-retransformation cycles are stress induced (**Fig. 6** (C)).

Together with a decreasing evolution of the resistance, **Fig. 6** (A) presents "stochastic" characteristics. See, for instance, the resistance evolution in b and c points associated to the same ageing temperature. With the aim of quantifying the evolution processes and eventually the "uncertain" effects, measurements at various constant temperatures have been carried out. From the series of observations, the existence of a relation between the time constant for the nearly-exponential evolution of resistance and the temperature has been observed, with an activation energy of 1.17 eV. The evolution of the transformation temperature after a temperature step (several hours or days) at room temperature implies an evolution in the state of order of the material and it could be considered that it is linked to the evolution of the B2 order, corresponding to the nearest neighbours atoms .

Once the steady state has been reached, the value of Ms is approximately linear with the ageing temperature T on parent phase (see the + + + on **Fig. 7** (A)). The slope value (dM_S/dT) approaches -0.105. The action of a temperature step near room temperature (from T_0 to

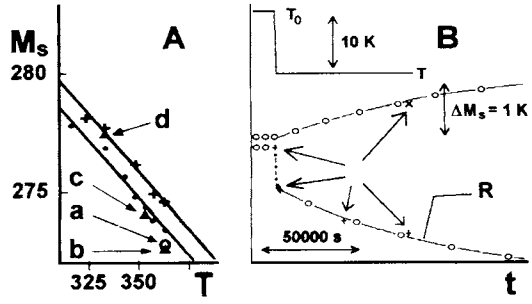

Fig. 7 A) M_S against ageing temperature; + + + first series of measurements; ● ● ● second series of measurements; a) after several partial times on 363 K, b) steady state on 363 K; c and d) other steady states; B) M_S and resistance behavior after a temperature step (from T_0 to T): [illegible] calculated values; (x or +) experimental values.

T) produces changes on transformation temperature: Ms displays nearly an exponential behaviour (see, **Fig. 7** (B)). Starting in a steady state at T_0, the Ms after a room temperature step (from T_0 to T) at time t_{ref} reads,

$$M_S(T, t) = M_S(T^0) + \Delta M_S^{B2}\,(1 - e^{-(t-t_{ref})/\tau^{B2}})\ ;$$

$$\Delta M_S^{B2} = -0.105(T - T^0)$$

with

$$\tau^{B2}/s = \exp\left(-29.304 + \frac{13630\ K}{T}\right)$$

The previous relations allow a predictive

Table 1 Relative time evolution of near-neighbours order: experimental and calculated effect on Ms (in K) after H hours ($H \equiv t - t_{ref}$) of a temperature step (from T^0 to T); experimental, predicted and difference δM_s; the T^0 value is 358.15 K.

H/h	T/K	M_s/K(exp)	M_s/K(calc)	δM_s/K
4.0	333.15	275.47	275.22	0.25
12.0	333.15	275.81	275.80	0.01
24.0	333.15	276.29	276.43	-0.13
59.4	305.65	275.28	275.23	0.05
59.4	293.15	274.83	274.93	-0.10

Table 2 Time-temperature effects on M_s; T^0 steady state temperature; T: actual temperature; H: elapsed time in days ($H \equiv t - t_{ref}$); b, c, d indicated on figure 7(A), (*) reproducibility of independent measurements; (†): asymptotic values (steady state conditions); δM_s: difference between experimental and calculated values.

T^0/K	T/K	H/day	Ms/K(exp.)		Ms/K(calc.)	dMs/K
	363.2	7(†)	272.52	b(*)		
	353.2	15(†)	274.02	c		
	333.2	26(†)	277.44	d		
	363.2	8(†)	272.32	(*)		
363.2	343.2	4.59	275.30		275.33	-0.02
345.7	325.5	10.1	277.30	A	277.52	-0.22
345.7	295.2	30.4	278.75	B	278.71	+0.04
345.7	295.2	55.8	279.06	C	279.05	+0.01

approximation to the values of the transformation temperature (see **Fig. 7** (B) and **Table 1**). The average difference (δM_s) between the calculated temperature and the experimental is less than 0.1 K in experiments lasting a few days.

The detailed observation of the resistance evolution for extended periods of time visualizes the LTT or Long Time Tail effects: a slight decrease in its value (41). Also, the relation between M_s and the ageing temperature is modified if the sample remains at "higher" temperatures (363 K) during a long period of time. After several hundreds of macro-cycles made up of an ageing of 9 hours at 363 K followed by ten cycles of transformation-retransformation the Ms changes to the point a in **Fig. 7** (A). Once the sample has spent 1008 ks (accumulated in five months) at a temperature of 363 K and, after 13 days at 333 K, the behaviour of Ms with regards to the ageing temperature is equivalent but decreased (see the points ● ● ● ● in **Fig. 7** (A)).

The long term analysis (LTT) allows for quantative estimates of the residual evolution of the resistance which can be associated to $L2_1$ order. From the experimental curves, a second time constant with an activation energy of 0.79 eV can be estimated. Departing from the experimental observations in LTT steady state (points b, c and d in **Fig. 7** (A)) an amplitude of M_s fluctuation is evaluated. Once the sample ***effectively*** finds a steady state at temperature T^0, the M_s after a temperature step (from T^0 to T) at time tref reads:

$$M_S(T, t) = M_S(T^0) + \Delta M_S^{B2}(1 - e^{-(t-t_{ref})/\tau^{B2}}) + \Delta M_S^{L2_1}(1 - e^{-(t-t_{ref})/\tau^{L2_1}})$$

with the same parameters for the "fast" B2 evolution, and, further:

$$\Delta M_S^{L2_1} = -0.067\ (T - T^0)$$

$$\tau^{L2_1}(s) = \exp\left(-16.933 + \frac{10330\ \mathrm{K}}{T}\right)$$

The time constant values associated with process $L2_1$ are very high: from 100 °C to 25 °C, the t^{B2} changes from 1400 s to 155 days and the related t^{L2_1} changes from 0.54 days to 1.6 years. The seasonal actions or summer and winter effects are then smoothed by the time constants value.

From the expressions associated to a Heaviside step after an steady state, it is possible to deduce the effect on M_s of a disturbance of the temperature or a Dirac pulse δT^0 produced in $t=0$. Starting on the previous steady state, the $M_s(\delta T^0, t)$ reads:

$$M_S(\delta T^0, t) = M(T^0) - \frac{0.105}{\tau^{B2}} e^{-t/\tau^{B2}} - \frac{0.067}{\tau^{L2_1}} e^{-t/\tau^{L2_1}}$$

Starting from a steady state seems possible to calculate the value of $M_s(t)$ produced by the evolutions of the room temperature with the use of a non-linear convolution. Preliminary reproducibility and reliability of the prediction for all effects are shown in **Table 2**. Starting at steady state at 345.7 K, the A, B and C values relate a long lasting "room temperature" evolution

with a cooling of 2 K day $^{-1}$ from 345.7 K to 295.2 K (final constant temperature). The quantification of the LTT effects allows for an increased reduction in the fluctuations on Ms in long lasting analysis. In general, the effects of the seasonal evolution of the temperature (summer-winter, *i.e.* greather than 20 K) affects the value of the M_s up to 17 % of the room temperature fluctuation (around 4 K) but the action is smoothed and delayed by the time constant values.

4. Conclusions

The particular behaviour of the SMA is associated with a phase transition between metastable phases. This implies the possibility of evolutions in the material. Its aplicability as a continous actuator with a long term guarantee requires an exhaustive quantification of its properties and subsequently, to mark out the limits of variability. Using high resolution equipment allows the carrying out of quantitive observations and to modelize its behaviour.

Using single crystals and single variant transformations allow for the quantification of the physical parameters of the process (nucleation, coalescence, friction between the interfaces, intrinsic thermoelasticity and the time coexistence effects), and to build a physical image model which supplies completely coherent results with the experimental observations. In the case of Cu-Zn-Al (electronic concentration 1.48 e/a), a recoverable evolution at low stress rates ($\leq$ 10kPa/s) is observed on the equilibrium temperature (around 0.7 K) when both phases coexist. This corresponds to the phenomena of martensite creep and micromemory.

To interpret the processes of ageing near room temperature only two ordering processes are required (for instance, B2 and $L2_1$ atomic orders). Starting from a steady state, it is possible to predict quantitatively the transformation temperature from the evolutions of the room temperature by means of a non-linear convolution. For the studied alloy, the yearly effects (summer-winter) of the room temperature fluctuations produce changes in the transformation temperature near 2 K. The applied working methodology to characterize the time dependence of SMA behavior has proved to be successful to reduce the stochastic components on transformation temperature M_s and to evaluate the particular parameters of the used alloy.

Acknowledgments: Cooperative research carried under contract NATO 920452. V.T. acknowledges CICYT, the key support of University of Provence and of FRMR and the partial support of ETSECCPB (cooperation program with the Dir. Pol. Territorial. Generalitat of Catalonia).

References

1) R. Newnham, Guest editor "Smart, very smart and intelligent materials," *MRS Bulletin* **18**, 24-25 (1993), and related articles in the same April 1993 MRS bulletin.

2) C. Friend, "Smart materials: the emerging technology," Materials World (January, 1996) 16-1

3) Proc. ACTUATOR 96, H. Borgmann Ed., AXON Technologie Consult GmbH (1996) Bremen, FRG.

4) C. M. Wayman, "Shape Memory Alloys," *MRS Bulletin* **18**, 49-56 (1993).

5) Proc. Comett Course, "The Science and Technology of Shape Memory Alloys," V. Torra Ed., Univ. Illes Balears (1989) Palma de Mallorca, Spain.

6) L. Delaey, "Diffusionless Transformations," Material Science and Technology, R.W. Cahn *et al.* ed., VCH, Weinheim, Germany, Vol.5 (1991) 339-404.

7) M. Ahlers, "Martensite and equilibrium Phases in Cu-Zn and Cu-Zn-Al alloys," Prog. Mater. Sci. 30 (1986) 135-186.

8) Proc. SMST'94, A.R. Pelton, D. Hodgson et T. Duerig Eds. MIAS (1995) Monterey, CA - USA.

9) Proc. ICOMAT'95, R. Gotthardt et J. Van Humbeeck Eds. J. Phys IV 5-C8 (1995).

10) F.C. Lovey, A. Amengual and V. Torra; "Experimental and crystallographic evidence for the growth of two equivalents β-variants from one single martensite plate in a Cu-Zn-Al single crystal"; *Phil. Mag. A* **64**, 787-796 (1991).

11) I. Müller and H. Xu, "On the pseudo-elastic hysteresis," *Acta metall. mater.* **39**, 263-271 (1991

12) J. Ortin, "Preisach modelling of hysteresis for a pseudoelastic Cu-Zn-Al single crystal" *J. Appl. Phys.* **71**, 1454-1461 (1992).

13) E. Patoor, A. Eberhardt and M. Berveiller, "Thermomechanical behaviour of shape memory alloys," *Arch. Mech.* **40**, 775-794 (1988).

14) B. Raniecki, C. Lexcellent and K. Tanaka, "Thermodynamic models of pseudoelastic behaviour of shape memory alloys," *Arch. Mech.* **44**, 261-284 (1992).

15) F. Marketz and F.D. Fischer, "Micromechanical modelling of stress-assisted martensitic transformation," *Modelling Simul. Mater. Sci. Eng.* **2**, 1017-1046 (1995).

16) F. C. Lovey, A. Amengual, V. Torra, and M. Ahlers, "On the origin of the intrinsic thermoelasticity associated with a single-interface transformation in Cu-Zn-Al shape memory alloys," *Phil. Mag. A* **61**, 159-165 (1990).

17) F. C. Lovey, A. Isalgue and V. Torra, "Hysteresis loops in stress induced ° -18R martensite transformations in Cu-Zn-Al," *Acta metall. mater.* **40**, 3389-3394 (1992).

18) V. Torra, "Shape memory alloys: from high-resolution thermal analysis to predictive modelling and simulation," *Thermochim. Acta* **200**, 413-426 (1992).

19) J. L. Pelegrina, M. Rodriguez de Rivera, V. Torra and F.C. Lovey, "Hysteresis in Cu-Zn-Al SMA: from high resolution studies to the time dependent modelling and simulation," *Acta metall. mater.* **43**, 993-999 (1995).

20) P. Y. Manach, "Étude du comportement thermomécanique d'alliages á mémorie de forme NiTi," PhD (1992), Institut National Polytechnique de Grenoble, France (in french).

21) Y. Gillet, "Dimensionnement d'élements simples en alliage á mémorie de forme," PhD (1994), ISGMP-Université de Metz, France (in french).

22) O. P. Bruno, "Quasistatic dynamics and pseudoelasticity in polycristalline shape-memory wires," *Smart Mater. Struct.* **4**, 7-13 (1995).

23) O. P. Bruno, P. H. Leo and L. F. Reitich, "Free boundary conditions at austenite-martensite interfaces," *Phys. Rev. Lett.* **74**, 746-749 (1995).

24) K. Nomura, S. Miyazaki and A. Ishida, "Cycling effect on the shape memory characteristics in sputter-deposited TiNi alloy thin films" in ref.3 pp.417-420.

25) M. Bendahan, "Réalisation et caractérisation de films d'alliage á mémorie de forme NiTi: Application á la réalisation de micro-actionneurs et de micro-capteurs" PhD (1996), Univ. d'Aix-Marseille III, France (in french).

26) R. Rapacioli and M. Ahlers, "The influence of short-range disorder on the martensitic transformation in Cu-Zn- and Cu-Zn-Al alloys," *Acta metal* **27**, 777-784 (1979).

27) A. Planes, J. Viñals and V. Torra; "Effect of atomic order on a martensitic transformation"; *Phil. Mag. A* **48**, 501-508 (1983).

28) J. Viñals, V. Torra, A. Planes and J. L. Macqueron; "The effect of atomic order on the thermodynamic properties of the martensitic transformation in CuZn and CuZnAl alloys"; *Phil. Mag. A* **50**, 653-666 (1984).

29) K. Tsuchiya, D. Miyoshi, K. Tateyama, K. Takezama and K. Marukawa, "Changes in the ordered structure of Cu-Zn-Al martensite by isothermal aging," *Scripta met. mater.* **31**, 455-460 (1994).

30) T. Tadaki, "Aging behavior of some shape memory alloys and its origin" in Shape Memory Materials'94, Chu Youyi and Tu Hailing Eds. (1994) International Academic Publishers, Beijing, pp.31-38.

31) Y. Dhazi and W. Zhongguo, "Aging effects of Cu-based shape memory alloys" in Shape Memory Materials'94, Chu Youyi and Tu Hailing Eds. (1994) International Academic Publishers, Beijing, pp.31-38.

32) T. Tadaki, Y. Nakata and K. Shimizu, "Occupancy sites of constituent atoms and their effects on the martensitic transformations in some Cu-based and Ti-Ni-based ternary alloys," J. Physique IV 5 (1995) C8-81-C8-90.

33) Y. Murakami, Y. Nakajima and K. Otsuka, "Effect of quenched-in vacancies on the martensitic transformation," *Scripta Materialia* **34**, 955-962 (1996) .

34) L. Buffard, "Influence des interactions, des défaults, de l'ordre-désordre et de la transformation martensitique sur l'hystérésis mécanique de l'alliiage á mémorie de forme Cu-Zn-Al-Ni" Ph D (1991) Ecole Centrale de Lyon, France (in french).

35) A. Amengual, A. Isalgue, F.C. Lovey, F. Marco and V. Torra; "Shape memory alloys: local and global transformations by high resolution thermal analysis"; *J. Thermal Anal.* **38** 593-602 (1992).

36) A. Isalgue, and V. Torra; "High resolution set-up for martensitic transformation in shape memory alloys. local studies in stress-strain-temperature," *Meas. Sci. Technol.* **4**, 456-461 (1993).

37) A. Isalgue, A. Torralba, and V. Torra, "From adapted and computerized thermomechanical equipment to modelling and time - evolution behaviour in Cu-Zn-Al shape memory alloys," *J. Thermal Anal.* **41**, 1425-1432 (1994).

38) A. Isalgue, H. Tachoire, A. Torralba, V. R. Torra

and V. Torra, "Predictable behavior of SMART materials (Cu-Zn-Al SMA) ," *J. Thermal Anal.* **47**, 151-163 (1996).

39) B-T. Chu, "Thermodynamics of deformation of solids" in Critical Review of Thermodynamics, E. B. Stuart *et al.*, ed., (1970), Mono Book Corp., Baltimore, USA, pp.299-343.

40) J. Malarria, M. Sade, and F. C. Lovey, "Bulk defects in pseudoelastically cycled Cu-Zn-Al single-crystals"; J. Physique IV 5 (1995) C8-889-C8-894 .

41) A. Isalgue, F. C. Lovey, J. L. Pelegrina and V. Torra, "Time evolution in static β-phase and dynamic β-martensite coexistence (Cu-Zn-Al SMA)," J. Phys. IV Coll C8 5 (1995) C8-853-C8-858.